frontiers in Materials

HYPOTHESIS AND THEORY
published: 30 April 2019
doi: 10.3389/fmats.2019.00089

Efflorescence of Alkali-Activated Cements (Geopolymers) and the Impacts on Material Structures: A Critical Analysis

Márlon A. Longhi[1,2], *Zuhua Zhang*[1,3]*, *Erich D. Rodríguez*[4], *Ana Paula Kirchheim*[2] and *Hao Wang*[1]

[1] Centre for Future Materials, University of Southern Queensland, Toowoomba, QLD, Australia, [2] Building Innovation Research Unit, Federal University of Rio Grande do Sul (NORIE/UFRGS), Porto Alegre, Brazil, [3] Key Laboratory for Green & Advanced Civil Engineering Materials and Application Technology of Hunan Province, College of Civil Engineering, Hunan University, Changsha, China, [4] Department of Structural and Civil Construction, Technological Centre, Federal University of Santa Maria, Santa Maria, Brazil

Even with the rapid development of the alkali-activated cement (AAC) technology in the past few years, some phenomena still needs to be better understood, that may alter the durability of the material. In many industrial uses and laboratory researches the formation of the salts on the surface alkali-activated type cements was observed, which was identified as efflorescence. This occurs due to the presence of an alkali transported in contact with the humidity and CO_2 environment. It may present externally from the formation of salts on the surface and internally with the carbonation of the alkalis in capillary pores. The effects of efflorescence on the material in use, as well as all factors that can influence its formation are not yet fully understood or reported. The search for papers was conducted using the search words efflorescence and geopolymer/alkali-activated, combined in the electronic data base. Due to the limited quantity of papers published related to efflorescence in geopolymers, the review was complemented using papers that discuss this behavior in Portland cement (PC) and based on the main properties that can influence the formation of efflorescence. In this paper, to understand the nature of efflorescence, upon which proper methods of minimizing of this issue can be based, the following aspects are discussed and re-examined: (1) the development of efflorescence's in PC concrete, (2) the role of alkalis in AACs, (3) efflorescence in AACs, and (4) effect from a physical and microstructural point of view of efflorescence's on the ACCs. This paper highlights that the nature of the pore structure and the design parameters (such as alkali concentration, presence of soluble silicates, and water content in the activator) are the two most important factors that control efflorescence rate and changes in mechanical behavior. However, the stability of the alkalis and their relationship with the formed gel, which are determining factors in the formation of efflorescence, remain not completely understood. In the same way, the effect of efflorescence in tensile strength and shrinkage needs to be evaluated.

Keywords: alkali-activated cement (AAC), geopolymer, fly ash, metakaolin, efflorescence, carbonation, durability

OPEN ACCESS

Edited by:
Andrew C. Heath,
University of Bath, United Kingdom

Reviewed by:
Mauricio Lopez,
Pontificia Universidad Católica de Chile, Chile
Jinrui Zhang,
Tianjin University, China

***Correspondence:**
Zuhua Zhang
Zuhua.Zhang@usq.edu.au

Specialty section:
This article was submitted to Structural Materials, a section of the journal Frontiers in Materials

Received: *18 November 2018*
Accepted: *09 April 2019*
Published: *30 April 2019*

Citation:
Longhi MA, Zhang Z, Rodríguez ED, Kirchheim AP and Wang H (2019) Efflorescence of Alkali-Activated Cements (Geopolymers) and the Impacts on Material Structures: A Critical Analysis. Front. Mater. 6:89. doi: 10.3389/fmats.2019.00089

INTRODUCTION

Alkali-activated cements (AACs), also broadly termed as geopolymers (mainly for those systems with low content of calcium), have been extensively studied in the past 40 years, due to the potential in the development of "green alternatives" to Portland cement (PC). The formation of geopolymers uses alkalis such as sodium hydroxide, silicate, and/or carbonate to activate aluminosilicates precursors usually heated clays, fly ash and slag, at room or elevated temperatures. The environmental benefit of applying AAC technology mainly lies in the reduction of CO_2 emissions and energy consumption, which are issues of wide concern for the sustainable development of the present cement and concrete industries (Damtoft et al., 2008). McLellan et al. (2011) pointed out that the unit emissions of greenhouse gas in making a geopolymer binder depend on the location of source materials, the energy source and the mode of transport. The counting of the four mixtures using typical Australian fly ashes indicated the potential for a 44–64% reduction in greenhouse gas emissions. Heath et al. (2014) showed that geopolymer manufacture can reduce CO_2 emissions by about 40% when clay minerals are used to replace fly, ash, and slag. In terms of weight, the manufacture of 1 m^3 of C25 (compressive strength of 25 MPa at 28 days) geopolymer concrete can reduce 154 kg of CO_2 emissions compared to using PC. This reduction will increase at a higher strength design (40 MPa geopolymer concrete reduces 220 kg of CO_2). The increase in the environmental impact can be related to the composition of the alkali-activator, where soluble silicate (such as sodium silicate) is the highest contributor. More recently, Passuelo et al. (2017), using a Brazilian calcined clay as precursor and a rice husk ash as part of the activator, reported that, per unit of compressive strength, the right design of material can provide a 50–75% reduction of CO_2 emissions. These have been one of the main forces driving the current research and industrial development of geopolymers.

Although the total volume of geopolymer concretes is negligible compared to OPC concretes, there has been rapid growth in the construction of demonstrative structures and buildings in the past decade because of increasing scientific research and environmental driving (Provis and Bernal, 2014). Notable examples are the 33 full-scale geopolymer concrete beams installed in the Global Change Institute building at the University of Queensland and the flooring of 40,000 m^3geopolymer concrete at Wellcamp airport, Queensland, Australia. From the challenges in supplying consistent raw materials and the cost issues, there are still a variety of technical and political barriers remaining, either unclear, or un-solved (Van Deventer et al., 2006, 2012). Efflorescence is one such problem which has been raised as a concern in some AAC formulations and this has been discussed briefly by Bernal et al. (2014), systematically investigated by Zhang et al. (2014c) and Zhang et al. (2018).

Looking back to efflorescence occurring in OPC based masonry and concrete, the most common phenomenon is related to the formation of calcium carbonate ($CaCO_3$) on the surface (Dow and Glasser, 2003). To avoid and mitigate efflorescence, the first principle is to reduce the alkali concentration of cements and also to reduce the solubility and absorption rate of CO_2 from the ambient environment (Dow and Glasser, 2003). However, in AAC systems, the concentrations of Na and K in pore solution usually contain much higher soluble alkali metal concentrations than conventional OPC based materials. Burciaga-Díaz et al. (2010) mentioned that alkali-activated slag based materials show significant efflorescence and some have also shown negative impacts on the mechanical properties. It must be noted that alkali-activated slag contains a higher concentration of calcium than alkali-activated metakaolin and fly ash systems, and this may lead to certain differences in the specific effects in the development of efflorescence. Škvára et al. (2012) assessed a set of fly ash-based geopolymers, where the acceptable workability and compressive strength above 40 MPa were achieved at a thermal curing (>50°C) and an alkali content of 30–150 g/kg, expressed as Na_2O to total mass of paste. These values are up to 42 times higher than in Portland cement paste (assuming 0.5% Na_2O in cement and w/c = 0.4 for paste). Therefore, this raises attention to the efflorescence issue in the application of AAC.

In literature and in the previous research done by these authors, a set of AAC mixtures developed efflorescence rapidly on drying surfaces when samples were in contact with water and under highly humid atmosphere conditions. A number of factors have been reported to affect the extent of efflorescence in AAC: alkali metal type (Škvára et al., 2009, 2012), raw materials (Temuujin et al., 2011; Kani et al., 2012; Bernal, 2016; Zhang et al., 2018), and reaction conditions (Burciaga-Díaz et al., 2010; Kani et al., 2012; Zhang et al., 2014c). However, there is still a lack of consensus relating to the mechanisms of reaction and formation, relationship between activator and reactivity, micro- and macro-structural impact of efflorescence and effective ways to mitigate.

Thus, the aim of this paper is to re-examine the results found in literature and complement the literature analysis with some ongoing experiments. The role of alkalis in AAC (low calcium systems) and the effect of alkali concentration on efflorescence are discussed. Particular interests are given to the different efflorescence behaviors of AACs that were prepared with fly ashes derived from different power stations, as well as calcined rich kaolinite clays. The importance of this issue is highlighted by the observations of the microstructural and mechanical properties of AACs that are subjected to efflorescence. The analyses and suggestions made here are based on the understanding of the effect of the curing scheme, design parameters, and reaction process of ACC, which is further related to reactivity.

EFFLORESCENCE IN PC CONCRETE

In Portland cement hydration process, the main constituents, the silicates C_2S (belite) and C_3S (alite) react with water to form the calcium silicate hydrates (C-S-H) and calcium hydroxide (CH, also named as portlandite). The CH is responsible for maintaining the high pH of concrete, which plays an important role in the compatibility between concrete and steel for reinforced concrete structures (Gallucci and Scrivener, 2007). The alkalis in PC concrete are generated into the system by the

hydration reaction of anhydrous components, including clinkers and supplementary cementitious materials (SCMs). SCMs are normally used as addition or substitution of cement (or clinker) to consume the content of $Ca(OH)_2$ and produce C-S-H via a pozzolanic reaction. On the other hand, the presence of CH within the concrete can promote its leaching, where part of this compound migrates to the surface and precipitates in contact with CO_2, forming a carbonate product as efflorescence. Other phenomena that can be developed is the internal crystallization due to the migration of soluble CO_2 from the environment into the matrix. The reaction of CO_2 with CH starts instantly and leads to formation of calcium carbonate (Cizer et al., 2012; Zhang et al., 2017). Further, other calcium phases are susceptible to carbonation (Garcia-González et al., 2006; Gallucci and Scrivener, 2007).

To understand the process related to the formation of whitish products, mainly efflorescence products, a model was proposed for Dow and Glasser (2003). According to the authors, efflorescence involves six basic and synergetic stages: dissolution of CO_2 (g) in H_2O at air-water interface on the surface of products, conversion of CO_2 to aqueous species, release of alkali(s), dissolution of $Ca(OH)_2$, diffusion of reactants through solution and precipitation of calcium carbonate, as shown in **Figure 1**.

According to the authors, in the first and second stages, the presence of another source of alkali such as NaOH or KOH may increase the dissolution of CO_2 and its absorption in the sample. It is related to the abundance of OH^- group in a high pH solution, which increases the reaction to form H_2CO_3. On the other hand, dissolved $Ca(OH)_2$ cannot increase the solubility, due to the insolubility of $CaCO_3$. In the third and fourth stages, the leaching of alkalis occurs, of which the main source is the cement itself. The content of $Ca(OH)_2$ is dependent on other factors as the type of cement, the use of SCMs, as well as the time of curing. Porosity is an important factor, according to Zhang et al. (2014a); while the reaction processes, the transport paths become longer if the matrix becomes more porous. The fifth stage is related to the diffusion, which is dependent on factors such as the pH of the pore solution, and the speciation of CO_2 adjusts to a new equilibrium amongst $(CO)_2$ (aqueous), H_2CO_3 and CO_3^{2-} and is then incorporated to the stages 1 and 2 and dissolved Ca^+ species. The final stage is related to the precipitation of $CaCO_3$ species.

The efflorescence in PC is usually observed in recent constructions and is not normally damaging, but, aesthetically undesirable (Dow and Glasser, 2003). However, it is necessary to evaluate the effect by the leaching process and the pore structure of the material, because this process can increase the porosity and accelerate the leaching. As efflorescence is a natural process, the material is exposed to evaporation. According to Dow and Glasser (2003), the efflorescence cycle can be interrupted by loss of liquid film by evaporation, perhaps combined with suction into porous material. During evaporation, the storage capacity of pure water for CO_2 is sufficiently low and the formation of efflorescence by complete evaporation makes a negligible contribution to efflorescence, relative to steady-state transportation. However, the concentrations of NaOH or KOH can increase the storage of CO_2. With this, even with evaporation, the content of CO_2 can increase during the wet/dry cycles. The efflorescence cycle can restart by reestablishment of a water film. The precipitated products may, depending on permeability and content of leachable alkalis, affect the reaction kinetics.

On the other hand, internal carbonation also induces a neutralizing effect to the highly alkaline environment provided by PC hydration (which in healthy/normal conditions shows a pH above 13 in pore solution), thereby increasing the vulnerability of embedded reinforcing steel to corrosion (Zhang et al., 2017). Internally, the effect is relative to crystallization process. According to Šavija and Lukovic (2016), there are two types of the carbonation process, (1) passive process when the carbonation causes unwanted and unplanned changes in the surface layer of a concrete structure or an element when exposed to the environment as pH drop, porosity changes, mechanical changes and cracking. However, (2) active carbonation assumes controlled exposure of cementitious materials to elevated CO_2 concentrations for certain periods of time, resulting in benefits in terms of mechanical performance or environmental impact of the material. The first one is attributed to deterioration and the second one to utilization. With this, it is evident that the process of carbonation and efflorescence is a complex subject even for PC-based materials, which have a great deal of related research. In fact, besides the reaction between CO_2, water, calcium and alkalis, efflorescence may also involve the reaction with cations sucked from the base of concrete embedded in saline soils and environment. This is a broad issue that occurs in many aging constructions.

ROLE OF ALKALIS IN AACs

When related to PC, ACCs present some peculiarities and differences in production process, raw material and reactions. AAC formation is a reaction between two parts of materials: reactive aluminossilicate powder (precursor) with a high alkaline solution (activator). The precursor presents negligible or no reactivity with water, and therefore it makes it necessary to introduce an alkali material to "activate" the precursor. It means that, the alkali placed in the system is necessary. The main reaction product of AAC is a disordered and highly reticulate structure named M-A-S-(H) gel (where M represents the alkali type, usually Na^+ or K^+) (Provis et al., 2005). The chemical process is well-known as alkali activation for CaO-rich systems or geopolymerization for CaO-free systems. This gel is a three-dimensional alumino-silicate network configurated of SiO_4 and AlO_4 tetrahedrons by oxygen bridges with positive alkali ions to compensate the negative balance of Al in a Q^4 molecular coordination (Provis et al., 2005; Fernández-Jimenez et al., 2006). However, just part of the alkali is bounded to the structure, the other part remains in pores (Provis and Bernal, 2014; San Nicolas and Provis, 2015), as proposed by the model of Rowles et al. (2007). According to the model, in a situation where there is sufficient amount of OH^-, Na^+ is bound superficially to the aluminate (**Figure 2A**). In situations where OH^- is not directly involved or accessible, Na^+ may associate with part of the silicon

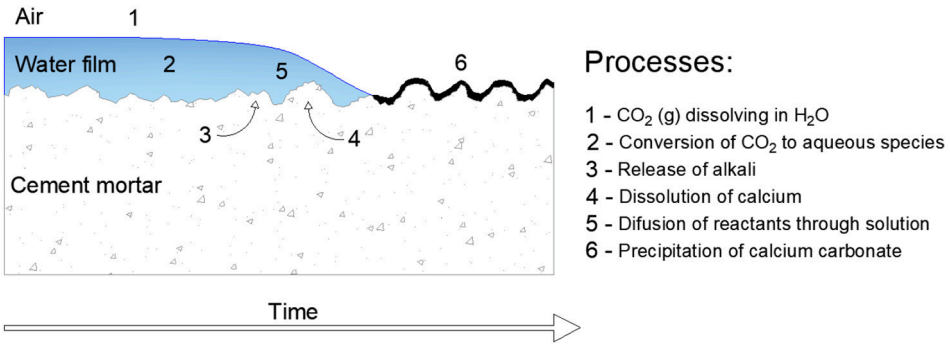

FIGURE 1 | Schematic process diagram for the formation of efflorescence of Portland cement concrete. Adapted from Dow and Glasser (2003).

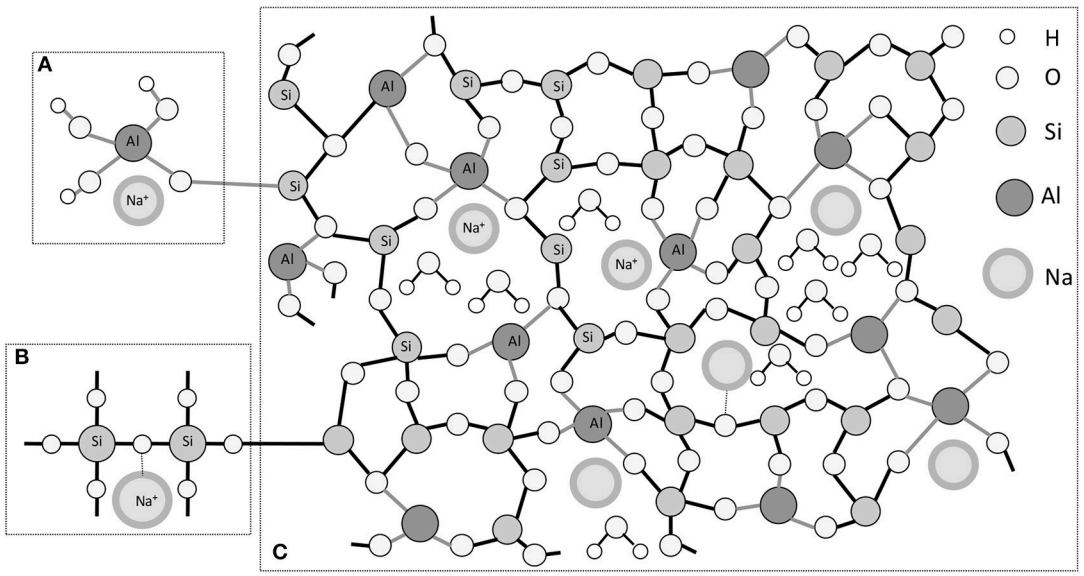

FIGURE 2 | Schematical model for aluminosilicates inorganic polymers adapted from Rowles et al. (2007). **(A)** Location of the charge-balancing Na^+ in form of a semiattached Na Aluminate species. **(B)** Location of the charge-balancing Na^+ cation in form of a modified brinding network. **(C)** Proposed schematic model for aluminosilicate inorganic polymers structure.

in the SiO-(Na^+)-Si^- form. In this situation, the negative charge of the AlO_4 tetrahedron can be located on the bridge with the oxygen atom, where Si-O-Si consequently generates the ionic bond with Na^+ (**Figure 2B**). In **Figure 2C** the model is fully represented, where in some points the ionic bonding with Na^+ occurs, but the other part of this element remains free in the pores of the structure.

According to Duxson et al. (2005), sodium can be linked with aluminum inside the gel structure, located within the pore solutions, neutralizing the charge of $Al(OH)_4^-$ group. Thus, sodium can be partially in the Na-O-Al(Si) form in the gel structure, with a relatively stronger Na-O bond, and partially in the form $Na(H_2O)_n^+$, with a weakly Na^+ associated with molecular water. This is aligned with the leaching result and deconvolution of ^{23}Na MAS NMR spectra for alkali-activated fly ash, assessed by Fernández-Jimenez et al. (2006). If it is assumed that the Na-O in gel structure is relatively more stable than in hydration conditions (contact with water molecules), similar to the Na-O in dehydrated zeolite, the soluble sodium must be limited, i.e., a certain fraction of sodium ions are not readily leached. Kani et al. (2012) grounded hardened AAC pastes and used stable leaching method at water to solid ratio of 20:1 to evaluate the leaching process. It was reported that after 24 h the leached alkalis were 1–7%, depending on the overall Si/Na and Na/Al molar ratios. Also, Zhang et al. (2014c) crushed hardened alkali-activated fly ash pastes (after 28 days of curing) into 1.25–1.5 mm particles. The authors used the stable leaching method at water/solid ratio of 25:1 and found that after 24 h the leached sodium was 12–16%, depending on the activator type, curing temperature, and amount of slag (added as a substitute for fly ash). These results are in agreement with the above hypothesis.

Škvára et al. (2012) crushed hardened AAC pastes after 28 days of curing and obtained particles under the size of 0.5 mm and used the dynamic leaching method (regularly change leaching

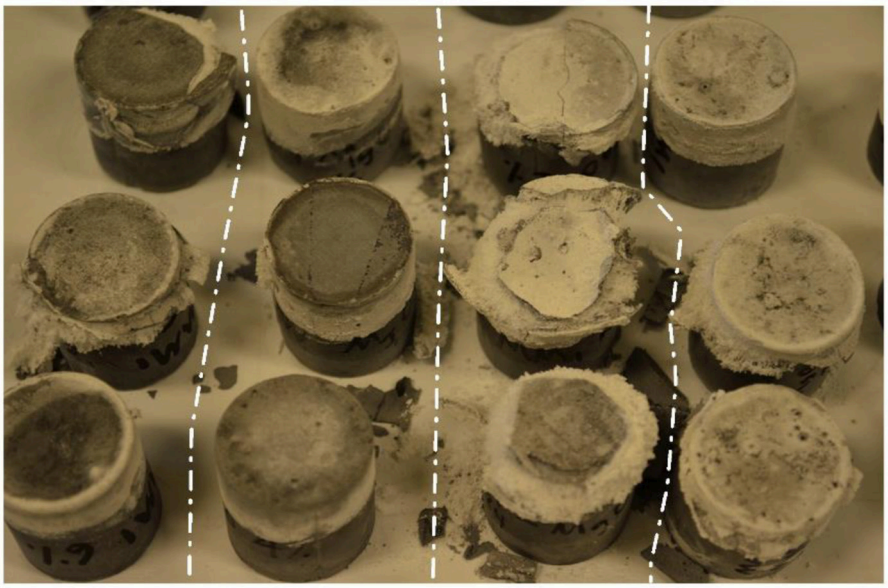

Mix design:
FA-6%MgO = Addition of 6% of MgO
FA-4%MgO = Addition of 4% of MgO
FA-2%MgO = Addition of 2% of MgO
FA-0%MgO = Addition of 2% of MgO

Production: Mixed 6 minutes at medium speed

Curing condition: 1 day sealed at RH = 90% ± 10% and 65 ± 1°C
27 days sealed at RH = 90% ± 10% and 25 ± 1°C

FIGURE 3 | Efflorescence formation in fly ash AAC with different contents of external MgO.

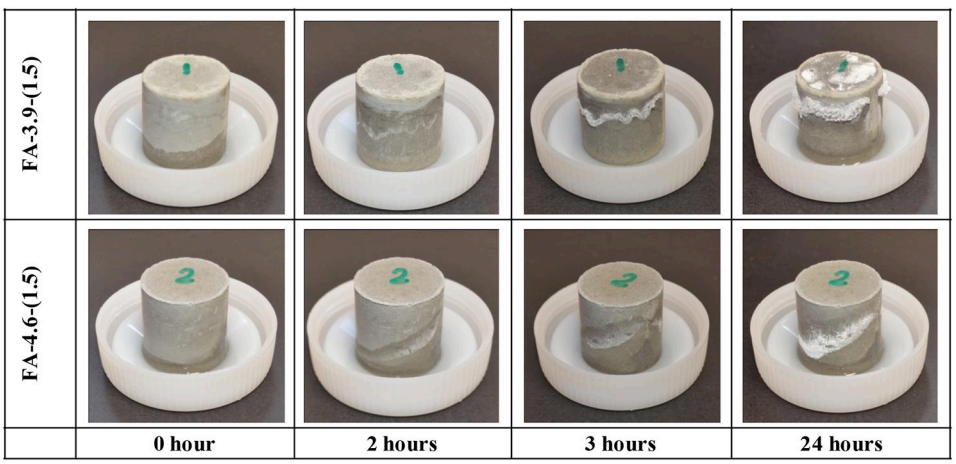

Mix design:
FA-3.9-(1.5) = 3.9% of Na_2O and MS content of 1.5
FA-4.6-(1.5) = 4.6% of Na_2O and MS content of 1.5

Production: Mixed 6 minutes at medium speed

Curing condition: 1 day sealed at RH = 90% ± 10% and 25 ± 1°C
12 hours sealed at RH = 90% ± 10% and 75 ± 1°C
5.5 days sealed at RH = 90% ± 10% and 25 ± 1°C

FIGURE 4 | Efflorescence of hardened alkali-activated fly ash pastes in contact with water. FA-4.6-(1.5).

solution with fresh water) and found that the alkalis can be almost completely leached from the binder after 150 days. In comparison with zeolite leaching behavior (usually extremely slow in water content), it was concluded that the alkalis (Na^+ and K^+) were only weakly bonded in the form of $Na(H_2O)n^+$.

However, some controversy about the leaching process was reported. Lloyd et al. (2010) measured the alkali concentration in the extracted pore solutions of typical ACC with 7% of Na_2O provided from activator. If it is assumed that all of the sodium presents in the form of $Na(H_2O)_n^+$ in pore solution, therefore, the followed analyses can be deduced: assuming 100 g of binder, the pore water (free water) is 10 g and the structural water is 5 g, and the sodium concentration is estimated to be higher than 20,000 mM. This value is far from the content identified by Lloyd et al. (2010), which were between 600 to 1,600 mM for alkali-activated fly ash systems. In fact, it is well-known that the alkalis bound in zeolite frame structure may have different states, and each state has its own ion exchange capacity. Therefore, a new hypothesis is proposed here: the alkalis in AAC have different states (maybe more than the two as was discussed above), and each state has its own leaching rate. If the alkali is available in pores of the material or it is weakly bounded, and the pores allow the movement of those alkalis, depending on the intensity and direction of this movement, different phenomena may occur, and will alter the integrity of the material.

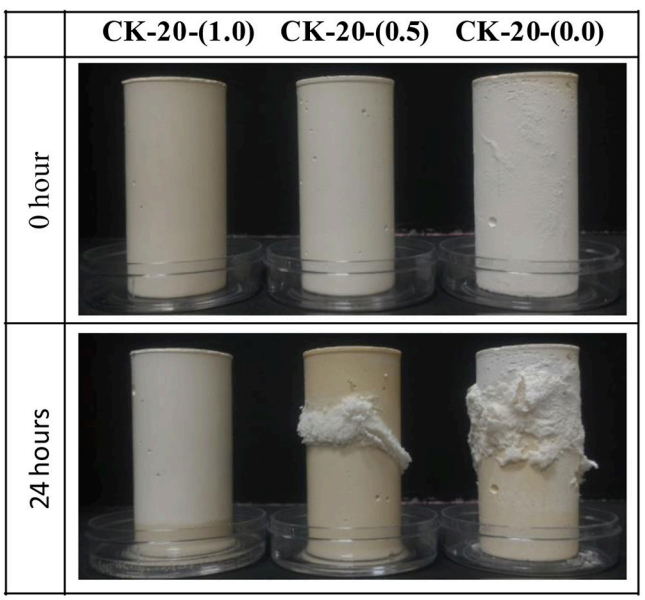

FIGURE 5 | Efflorescence of hardened alkali-activated calcined kaolin pastes in contact with water. CK-20-(1.0) means 20% Na_2O in terms of mass ratio to calcined kaolin, and MS is 1.0.

EFFLORESCENCE OF AACs

During the last few years of rapid development and application of AAC technology, the formation of depositions of material was observed on the surface of the samples. This was initially observed in laboratory conditions and later began to receive attention (Škvára et al., 2009; Kani et al., 2012; Bernal et al., 2014; Zhang et al., 2014c, 2018; Yao et al., 2015). This phenomenon is the result of a chemical reaction between free leached alkalis in porous structure with CO_2 in the aqueous form, where alkalis are the result of a physical leaching process, i.e., this only happens when alkalis are free to transport. With this, alkali leaching is relative to the amount of free cations and movement facility within the porous structure. These factors are dependent from synthesis conditions and the reacted products formed after the alkali-activation.

The Relation Between Alkali Leaching, Design Parameters, and Activation Products

The first design parameter is related to precursor. The most used are fly ash, metakaolin, and ground granulated blast-furnace slag (GGBFS). All of them have a specific chemical composition, with different oxides content, particle size and geometry, which changes the properties and features of the final reacted product. The reactivity has a wide behavior due to an internal factor of the material that depends on its generation process. In this regard, particle size has an important function, since smaller particles have a larger specific surface area and consequently a higher initial reactivity. A more reactive material can usually provide a denser matrix, with less porosity. Systems with fly ash and metakaolin are known as low calcium, while granulated blast furnace slag is known as high calcium precursor. In low calcium systems, the molar ratio SiO_2/Al_2O_3 is an important indicator of the initial reactivity and microstructural features of the gel formed. According to Criado et al. (2007), the Si-O bond is stronger than the Al-O bond, and this influences the precursor dissolution process, which result in an easier dissolution to precursor with higher content of Al_2O_3. This relation also alters the final product, that is Q^4 linked with different degrees of Al substitution (Duxson et al., 2005). Relating this to the Rowles et al. (2007) model, more Al content is believed to result in the higher imprisonment of Na^+.

Precursor with high calcium content exhibits a different behavior. Usually, this material needs less content of alkalis for its dissolution. Also, the gels formed are different from low calcium gels. While low calcium presents the M-A-S-(H), high calcium systems presents gels calcium aluminosilicate hydrate (C-A-S-H). According to Provis and Bernal (2014), this type of product possesses a disordered tobermorite structure in layers of coordinated silicon tetrahedral, where the interlayer region contains Ca^{2+} cations, alkalis, and the water chemically incorporated into their molecular structure. This is important for the alkali leaching because cations incorporated into the gel are less leachable in a system where water is also attached to the structure and does not work as a transport agent. Zhang

et al. (2014c) assessed the efflorescence in geopolymeric systems (free calcium AAC) activated by the use of NaOH and sodium silicate as activators, where a significant reduction of the means particle size and porosity with GGBFS addition was observed, reducing the susceptibility of efflorescence development. When slag is introduced in metakaolin or fly ash systems, the products may contain hydrotalcite-like phases, which have been proven to have ion binding properties. However, there is no report on this aspect, which deserves future insight study.

Besides the addition of slag, a certain amount of MgO in alkali-activated metakaolin-based geopolymers (Zhang et al., 2012) and slag/fly ash-based geopolymers (Shen et al., 2011) have shown benefits of reducing autogenous shrinkage and drying shrinkage. An experiment of adding MgO in ambient cured sodium silicate-activated fly ash-based geopolymers has been conducted to examine its effect on efflorescence. **Figure 3** shows the appearance of sodium silicate-activated fly ash ACCs with different amounts of MgO. When MgO is used between 2 and 6%, the efflorescence behavior does not show a consistent trend. After 2 weeks in contact with 2 mm-deep water at bottom and naturally drying at the ambient conditions (20 ± 10°C, RH = 50 ± 20%), the control samples without MgO have sever efflorescence products formed on the surface, while the samples with 2 and 6% MgO show more severe efflorescence, and the products formed under surface lead to enough crystallization stress to break the top surface of the sample. Interestingly, the sample with 4% MgO addition have slower and much less severe efflorescence. This behavior indicates that efflorescence is a complex function of the raw materials, the minerals and the microstructure of the products. The risk of adding MgO in low calcium geopolymers must be considered.

About the activators, the most usual are sodium and potassium in the form of hydroxide and silicate. Commonly both materials are used combined and the addition of silicates increases the content of soluble silica in the activator, which enhances the compactness of matrix (Zhang et al., 2013; Longhi et al., 2016). As molar ratio is used to characterize the activation content, M_2O/Al_2O_3 represents the fraction between the activator oxide and the Al_2O_3 content of the precursor. This relationship is determined by the stoichiometric equilibrium, where in a fully reacted precursor, each Na^+ can connect with an $[AlO_4]^{5-}$, establishing an ionic bond (Rowles and O'Connor, 2003; Duxson et al., 2007). In an ideal system, the unit value indicates the consumption of all Na^+ cations. According to Zhang et al. (2013), when Na_2O/Al_2O_3 <1, the increase in NaOH concentration is effective in increasing the extent of the reaction, however, values higher than 1 indicate excess of Na^+, which will not establish connections and will be free in the structure. This part is prone to form efflorescence. However, the results reported by Kani et al. (2012) showed that the extent of leaching alkalis improved with Na/Al increasing from 0.61 to 1.23, and the susceptibility in the development of efflorescence of dry samples after immersion. Although, for this relationship to be chemically possible, during the design process it is important to consider the reactive (or reacted) part of precursor, because other fractions will just work as inert filler. In the same way, a different activation design will provide different values of dissolution and reaction, with changes in the effective content of oxides in the geopolymer gel. The relation between design parameters, amount of gel formed, and alkali stability is an important topic to be approached and better understood, and is directly associated with efflorescence formation.

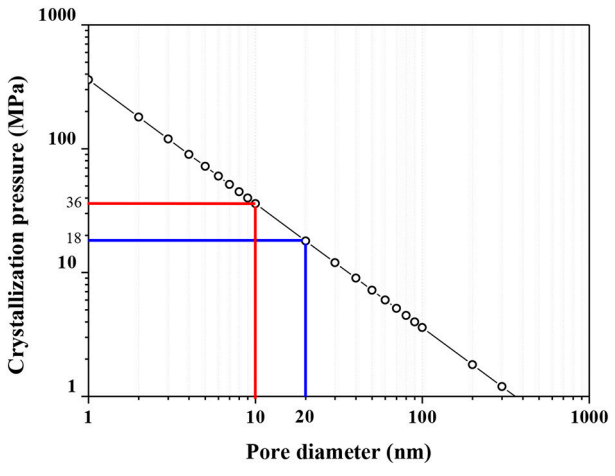

FIGURE 6 | Crystallization pressure as a function of the diameter of a cylindrical pore.

Another important factor is related to the curing process. The increase in the temperature promotes the reaction and dissolution of oxides and the acceleration of the kinetics of geopolymerization reactions (Granizo et al., 2014). This factor was also evaluated for the formation of efflorescence. Kani et al. (2012) observed that the curing temperatures higher than 65°C provided a significant effect in efflorescence reduction and also higher compressive strength using natural pozzolan. This behavior was also verified by Zhang et al. (2014c) from the use of fly ash as precursor and then cured at temperatures between 25° and 80°C. The use of thermal curing is effective to precursors with low reactivity and its effect can be attributed to a higher amount of gel formed with associated higher density and higher amount of imprisoned Na^+.

The information discussed above has shown that activator type and curing conditions are likely to be the critical aspects in the development of efflorescence, and this has been backed up by experimental data. **Figure 4** shows experiments where the rate of efflorescence development was assessed using fly ash-based as precursor [FA-**3.9**-(1.5) and FA-**4.6**-(1.5)] and **Figure 5** shows experiments using calcined kaolin [CK-20-(**1.0**), CK-20-(**0.5**) and CK-20-(**0.0**)]. The fly ash-based geopolymers were prepared by the activation of sodium silicate (SS) solution at different dosages: FA-**3.9**-(1.5) contained 3.9% Na_2O (expressed as Na_2O to fly ash mass ratio, excluding the Na_2O originating from fly ash) and Ms value of 1.5 (molar SiO_2/Na_2O ratio in the activator), while FA-**4.6**-(1.5) contained 4.6% Na_2O and Ms values of 1.5. The fly ash samples were cured in sealed molds for initial 24 h at RH = 90 ± 10%, 25 ± 1°C, followed by 12 h curing at 75 ± 1°C and naturally cooled down to 25 ± 1°C and allowed further 7 days of aging. Specimens were removed from molds and put in ambient air with the bottom immersed

in water at a depth of 0.5–1 mm. The efflorescence occurs on the surface of FA-**3.9**-(1.5) more rapidly: tiny white products are observable after 1.5 h (not presented here), and after only 2 h, evident efflorescence products can be seen on its surface above the wet line. In comparison, FA-**4.6**-(1.5) starts to exhibit visible efflorescence after 2 h. The leaching analysis of the crushed samples, as a quantitative method of assessing efflorescence potential (Zhang et al., 2014c), shows that the two AACs have very close sodium releasing rate and fraction (not shown). It means that FA-**4.6**-(1.5) has higher efflorescence potential as the absolute amount of leached alkali is higher. This result indicates that lowering the alkali concentration in an AAC by reducing the amount of sodium silicate activator may not be a good practical method to mitigate efflorescence. In fact, other factors, such as gel

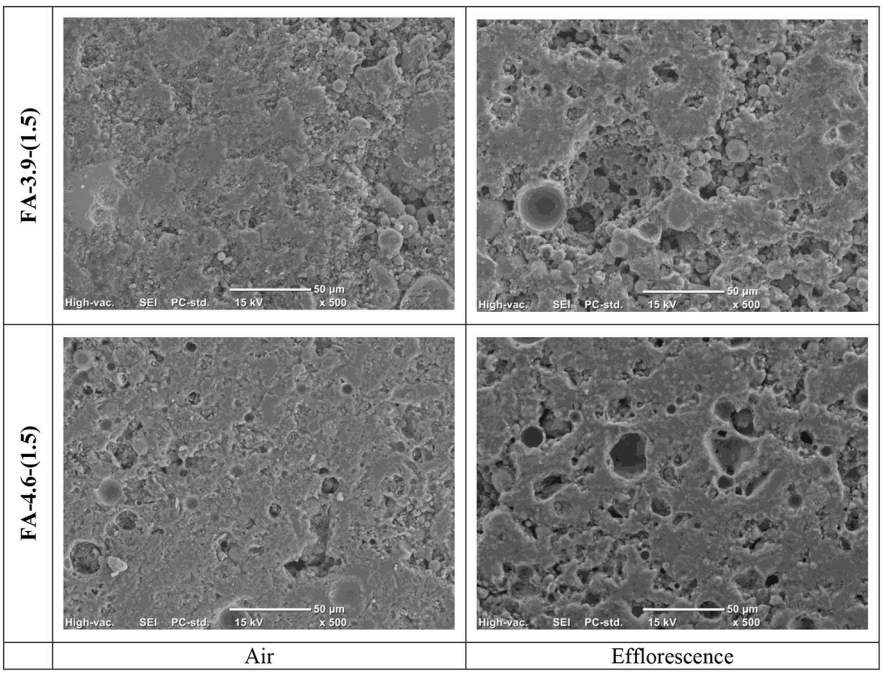

FIGURE 7 | Scanning electron micrographs of AACs after 28 days of aging under ambient air and accelerating efflorescence conditions.

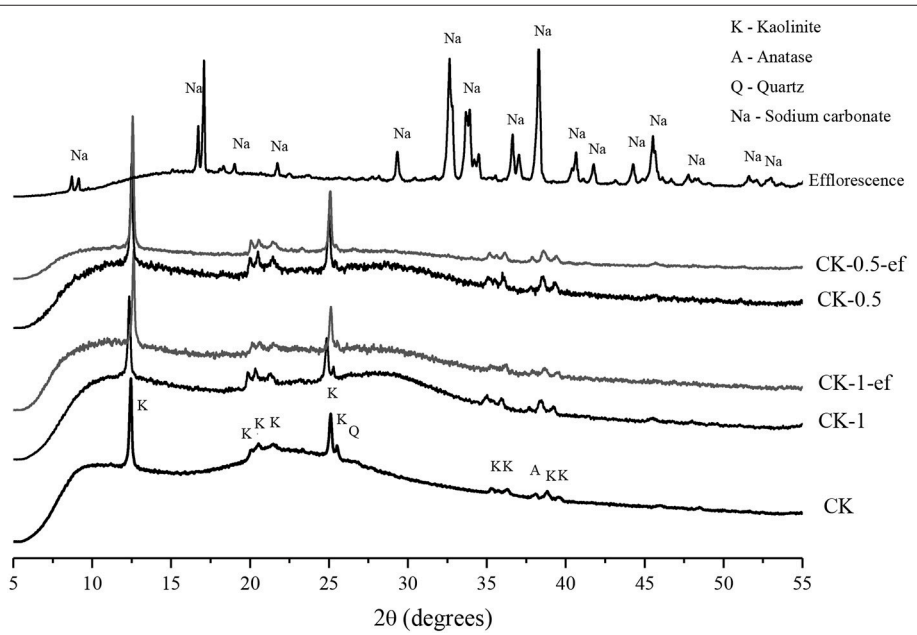

FIGURE 8 | XRD analysis of precursor, CK-bases geopolymers before and after efflorescence formation and efflorescence product.

composition (as a result of varied reaction extent of fly ash due to the change of activation conditions) and the pore features (size and volume), can also influence the efflorescence rate.

Figure 5 shows experiments on calcined kaolin-based geopolymers (CK). This material was activated with sodium silicate and NaOH, with fixed 20% of Na_2O and different MS values: CK-20-(**1.0**) with MS = 1.0, CK-20-(**0.5**) with MS = 0.5 and CK-20-(**0.0**) with MS = 0.0 (NaOH-based geopolymer without any soluble silicate in the activator). The CK samples were cured for 28 days at RH = 90 ± 10% and 25 ± 1°C in a sealed plastic container. Specimens were removed from molds and partially immersed in distilled water (at a depth of 5 mm). The system with MS = 1 did not show efflorescence even after 28 days of assessment (not shown here). With MS = 0.5 after 1 day, it was able to clearly identify a layer of efflorescence from the middle of the sample. For the system with MS = 0, the efflorescence was observed even before contact with water, where the leaching was observed due to the internal moisture of the test specimen. After the immersion, an increase in the formation of efflorescence was rapidly identified. This makes it evident that the effectiveness of silicate is soluble when used as activator. In this sense, the system that did not show efflorescence also presented higher mechanical (∼52 MPa at 28 days) behavior. Another factor to be considered when comparing with fly ash systems is that the amount of activator required for calcined clay-based geopolymers is usually two to three times higher.

The Difference and Similarities Between Efflorescence and Subflorescence

Crystallization process is the opposite to the solubilisation of a solid. In a solution when saturation is exceeded, part of solute will be separated from the solution and precipitates as solid crystals to keep the solution saturated. As shown previously, after the leaching process, the alkalis are brought to the surface and are crystallized by the carbonation process, generating efflorescence. However, according to Scherer (2004), porous material can be damaged when crystal precipitate from the liquid in their pores. The size of the pores and the magnitude of the repulsive force between the salt and the confining pore surfaces are also important factors. In turn, supersaturation is dependent on the nature of the salt, the rate of the supply of the solution and the evaporation of water (Scherer, 2004). In this way, the crystallization can occur in two ways: efflorescence, when the internal alkalis are carried toward the surface, providing Na^+ for the precipitation of sodium carbonates, until an equilibrium (saturation) condition between the pore solution and the crystals is reached (Zhang et al., 2018); or subflorescence, when the crystallization occurs within pores (Dow and Glasser, 2003), in a depth sufficient to allow the absorption of dissolved CO_2. According to Zhang et al. (2018), efflorescence and subflorescence are both related to the carbonation process, however, the material properties, exposition, and environment can determine what will be formed.

Regarding porosity, in a porous material, water is draw up by capillary pressure, which is dependent on the pore size distribution. The flux ($J = -\kappa.\Delta\rho/\eta$) into the porous material is given by Darcy's law, and is dependent on permeability (κ), viscosity (η), and pressure (ρ). To balance the system, water raises between the pores until an equilibrium height is achieved. In the evaporation process, the internal water of pores is brought to surface and reduces the height of equilibrium. When there is the presence of dissolved salts, as water evaporates, the concentration of salt in the liquid rises and the salt concentration at the drying surface until the supersaturation are high enough to cause the salt precipitation (Scherer, 2004). Summarizing this, the water will be transported into the material by capillary pressure. With the evaporation process, the transported salts are precipitated in a spatial sequence according to the ion activities of the salt phases in the system (Arnold and Zehnder, 1989). However, above the evaporation region, as well as throughout the inner part, due to the presence of remaining soluble salts, is the subflorescence zone. In AACs, if a soluble carbonate is available, it can be transported to the inside and enable the crystallization of the salt, which in this case is a carbonate, and the resulting crystallization pressure may exceed the tensile strength of the material (Scherer, 2004).

In the crystallization process, every salt has an equilibrium relative humidity, which is also relevant to the ambient humidity and temperature. If the relative air humidity is lower than the equilibrium humidity of the salt (RH < Hr eq), the salt will

FIGURE 9 | Sample with calcined kaolin as precursor and activated with 10% of Na_2O from NaOH with visible surface deterioration.

crystallize. Correlating this with AACs, when RH is low, with the availability of a hydrated carbonate provides a movement to inside structure, which may crystallize internally with the contact with free alkali. If the relative air humidity is higher than the equilibrium humidity of the salt (RH > Hr eq), the salt dissolves and can be brought to the surface by a transport agent. This means that the relative humidity of the environment and salt crystallization will define whether there will be efflorescence or internal crystallization (subflorescence). The equilibrium humidity of a specific salt is not always available or has never been evaluated; however, the carbonate Na_2CO_3:$10H_2O$, at 25°C, presents Hr eq of 88.2% (38). In the same way, the capillarity will determine the rate of water movement and aqueous CO_2 movement and consequently the depth of subflorescence.

In literature that evaluated the formation of efflorescence in AACs, the main products formed are sodium carbonates. The formation of a hydrated carbonate ($Na_2CO_3.7H_2O$) was observed by Škvára et al. (2009) and Zhang et al. (2014c), sodium bicarbonate ($NaHCO_3$) by Kani et al. (2012) and natrite (Na_2CO_3) by Burciaga-Díaz et al. (2010). In a system with potassium as activator, it is possible to form potassium carbonate (K_2CO_3) or hydrated potassium carbonate phases, however, this last one does not give rise to visible hydrates as postulated by Škvára et al. (2009), and for this reason, the use of potassium could be indicated for the reduction of efflorescence (or efflorescence visibility). Even without visible efflorescence formation in geopolymers based on potassium as main activator, the leaching process of this element can allow the removal of alkalis and cause microstructural damages.

In short, efflorescence is the crystallization process of alkalis leached from the AAC matrix in contact with aqueous carbonate solution in a reaction format as follows Zhang et al. (2014c).

$$CO_2(g) + 2OH^-(aq) \rightarrow CO_3^{2-}(aq) + H_2O$$
$$2Na^+(aq) + CO_3^{2-}(aq) + 7H_2O \rightarrow Na_2CO_3.7H_2O(s)$$

According to Zhang et al. (2014c), this is therefore a partial neutralization for alkaline geopolymers under natural carbonation conditions, as dissolved CO_2 acts as an acid and consumes hydroxides. The main reason for efflorescence in these materials is the availability of mobile Na^+ and OH^-, which are related to the material permeability. In a situation with very aggressive leaching, it can also remove the equilibrium cation (Na^+) and destabilize the aluminum tetrahedral, which may damage the matrix structure. This mechanism, however, has not been solidly verified nor highlighted to date.

Internally, the carbonation process may follow the same reactions, but its effect could be different. The formed crystal can be expansive which induces internal stresses. The stress in the megapascal range is only expected in nanometric pores, and lower pressure in larger pores. This pressure can be mechanically damaging depending on the pore structure. According to Scherer theory (Scherer, 2004), the supersaturation of salts can result from capillary rise and evaporation, or from cycles of wetting and drying. In contact with water, the humidity in the pores is expected to be very high, which support the formation of $Na_2CO_3{\cdot}7H_2O$ as detected by Zhang et al. (2014c).

To predict the relation between crystallization pressure and pore diameter, using the estimated liquid interfacial free energy ($\gamma_{CL} = 0.09$ N/m) of $Na_2CO_3{\cdot}10H_2O$ (Rijniers et al., 2005) and Equation 1 that describes the pressure in a confined spherical crystal with radius of r as proposed by Scherer (2004), it is possible to estimate the crystallization pressure in a cylindrical. The relation between crystallization pressure and pore diameter is shown in the **Figure 6**.

$$p = 2\gamma_{CL}/r \quad (1)$$

As reported in some previous papers (Škvára et al., 2006; Van Deventer et al., 2006; Zhang and Wang, 2016), the pore sizes in geopolymers determined by mercury intrusion are at a range of several nanometres to 2,000 nm. In an experiment conducted using different contents of fly ash and metakaolin, (Zhang et al., 2014b,c) observed the concentration of 80–90% of the pores smaller than 20 nm. The crystallization process inside a pore of 20 nm can generate a pressure of 18 MPa and 36 MPa for 10 nm pores. The pressure increases in an exponential relation to the pore diameter. Large pores can permit the growing of crystal with a low crystallization pressure, however, the crystal formation in small pores can generate a high pressure (Longhi et al., 2016). The impact on the integrity of the samples, and particularly whether the process will be harmful or harmless, depends on the magnitude of the crystallization pressure compared to the tensile strength of the geopolymer matrix (Zhang et al., 2018).

IMPACTS OF EFFLORESCENCE ON AACs

Microstructural Impacts

So far, there has been very limited structural analysis reported in literature related to the formation of efflorescence in ACC. Zhang et al. (2014c) analyzed the pore structure by scanning electron microscopy (SEM), and made some important considerations. The leaching process is related to the pore size distribution where a large pore induces a faster alkali leaching.

The effect of efflorescence on the microstructure of the same material showed in **Figure 7**, FA-**3.9**-(1.5) and FA-**4.6**-(1.5), is

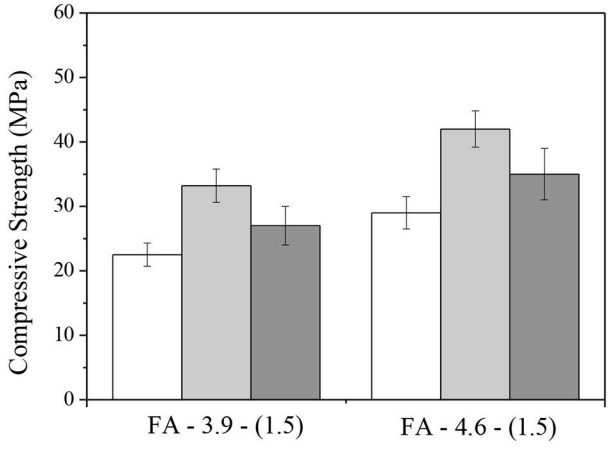

FIGURE 10 | Compressive strengths of well-matured fly ash AACs after demoulding, air-aging and accelerating efflorescence for 28 days.

shown in **Figure 7**. The images correspond to the surface parts of each sample after 28 days of ambient aging (in the air) and accelerating efflorescence (with bottom immersed in water as described above). The crushed particles near surface were solidified using resin, polished, and washed in acetone using an ultrasonic washer to remove loose particles.

After the accelerating the efflorescence procedure, FA-**3.9**-(1.5) becomes more porous when compared to the corresponding samples. The same polishing and washing procedures were used for all samples; the porous microstructure in cross-section implies that the binder may be softer or less strong as a consequence of the development of efflorescence. The cross-section of FA-**4.6**-(1.5) after the accelerating efflorescence program shows the same microstructural feature. Zhang et al. (2018) implied that one of the reasons for the increase in large pores is that the later reaction was affected in the specimens with efflorescence, due the consumptions of alkalis to form de $Na_2CO_3 \cdot nH_2O$, reducing the ongoing reaction of gel.

Trying to understand the microstructural effect of efflorescence, Zhang et al. (2018) evaluated the T-O (T = Al or Si) bonding environments by FTIR spectroscopy in systems with intense efflorescence in contact with water. The authors observed a shift of the main band as well as a lower intensity in the systems in contact with water when compared with those samples in air. The author also indicated that efflorescence in geopolymers does not change the main mineralogical composition of the binder, however, it restricts the later reactions, which is expected to be harmful to the strength development. Unfortunately, the actual mechanical testing on tensile strength change was not reported in the previous study.

Figure 8 shows XRD results of the CK-based geopolymers as presented in **Figure 5**. The first diffractogram represents the precursor, a calcined kaolin (CK), which shows the presence of kaolinite, anatase, and quartz. The hump between 19 and 28 degrees is attributed to the amorphous feature of metakaolin. After the geopolimerization process, another hump is visible between 26 and 34, and attributed to the gel formation. After the efflorescence process, it is able to identify a hydrate sodium carbonate ($CaCO_3.nH_2O$). The formation of such carbonate may be from the carbonation of calcium solution as the calcined kaolin contains a certain amount of CaO as impurity, which becomes available after alkali-activation. The system CK-20-(1.0) shows 34.8% of crystalline content, and after the efflorescence process it becomes 41.4%. The system CK-20-(0.5) presents 39.7% before and 49.7% after efflorescence. This degree of crystallinity was obtained by mathematical peak deconvolution. This increase is visible by the reduction of the main hump near to 28° in 2θ. This means that there is a reduction in the material amorphic structure after the efflorescence.

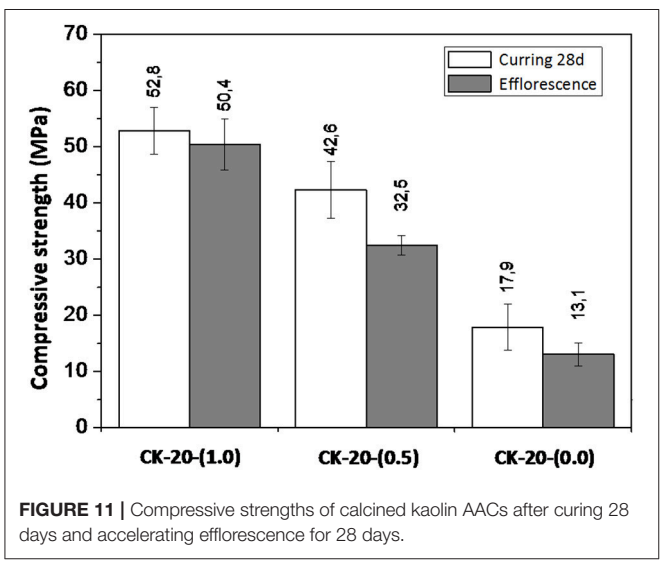

FIGURE 11 | Compressive strengths of calcined kaolin AACs after curing 28 days and accelerating efflorescence for 28 days.

Due to the formation of the carbonate crystal, microstructural changes become visible in sample integrity. In some systems, after wetting and drying cycles, the process of dissolving alkalis is followed by evaporation of the water, which allows the movement to surface, and it causes severe deterioration. **Figure 9** shows a sample produced with the CK subjected to contact with water at the bottom in an environment with ∼50% RH, so that the movement of water and alkalis by evaporation was forced. The excess of leaching or/and the crystallization in superficial pores may cause this deterioration.

Mechanical Impacts

Burciaga-Díaz et al. (2010) evaluated how different formulations affected the development of compressive strength, and found that in slag-based AAC, the addition of more than 5% of Na_2O decreased the compressive strength. This effect was attributed to the excess of alkalis and the consequent efflorescence formation, which was visually observed. In the same work, however, when MK was added as a precursor, it required a larger amount of Na_2O (15%), while no reduction in the mechanical properties was observed, nor any efflorescence.

In a long-term exposure for a fly ash-based AAC, Škvára et al. (2012) observed reduction in compressive strength for the water immersed samples when compared with those exposed to air. However, this reduction was attributed to the higher cohesion forces between the gel particles in the dry concrete. To the same authors, as it was found that Na^+ was replaced by H_3O^+, Škvára et al. (2009) argued that a large part of Na are bounded in the form of $Na(H_2O)_n^+$, rather than ironic bonds -O-Na^+. It should be noted that in this specific case, the immersed sample only lost the alkalis by leaching, and no crystallization process occurred.

The mechanical properties of fly ash-based geopolymers by different periods of curing, and types of exposure were evaluated by Yao et al. (2015). By comparing the compressive strength results, it was found that the immersed samples and those submitted to bottom contact with water (accelerating efflorescence) presented lower values compared to the control samples that were left in air. The time of exposure also contributed to the strength reduction. The negative effect of immersion was attributed to the instability of sodium aluminosilicate gel in water. For the samples with bottom contacting water, the formation of carbonate crystal and microstructure damage was believed to be the main factor to the reduction of mechanical behavior. In terms of linear shrinkage, the shrinkage of the samples immersed was smaller than that of

efflorescence samples due to the availability to free water in the binder under the immersion condition.

As observed by Yao et al. (2015), the environment of exposure is an import factor that affect carbonation process. A direct comparison by measuring the specimens after demoulding, air-aging, and accelerating efflorescence were recently made by the authors. **Figure 10** shows the compressive strengths of the fly ash-based AACs, the same as presented in **Figure 2**. After 28 days of aging, the compressive strengths of the pastes in air showed an increase by 20–35% compared with that at demoulding age, while the efflorescence samples showed smaller increase.

Calcined clays-based AACs were also evaluated by compressive strength (**Figure 11**). The samples identified as CK-20-(**1.0**), CK-20-(0.5), and CK-20-(0.0) were the same as presented in **Figure 3**. After 28 days of curing in a sealed plastic container at RH = 90 ± 10% and 25 ± 1°C, followed by 28 days more in contact with water to accelerate efflorescence formation, it was found that the first system [CK-20-(**1.0**)] showed less susceptibility of efflorescence, and this behavior is attributed to the denser and stronger structure which provides a lower water absorption, and consequently a lower movement of alkalis to the surface. The other systems presented strength reductions of ∼25% and extensive effloresce formation. Thus, it is able to confirm that the mechanical behavior and its susceptibility to efflorescence formation in these systems are related to the design parameters.

Therefore, it is evident that the efflorescence has a negative influence on the strength development. When an AAC paste is placed in accelerating efflorescence conditions, water can be drawn into the pores of the solid matrix by capillary suction and evaporate from the sample surface. The internal alkalis are able to diffuse toward the surface, providing Na^+ for the precipitation of sodium carbonates, until an equilibrium (saturation) condition between the pore solution and the crystals is reached. The reduced alkali concentration in the matrix, due to diffusion, will affect, or suppress the later activation of residual precursors. In addition, the crystallization pressure due to the precipitation of sodium carbonates in the pores of binder may also introduce inner stress, which consequently affects the mechanical properties of AACs.

CONCLUSIONS

Even with the recent advances in AAC technology, the understanding of the efflorescence phenomenon is still a knowledge gap and is distinct from that which occurs in PC-based materials. Some progress has been made to understand these efflorescence mechanisms and the factors that influence them, but some topics need to be better clarified. Based on the previous researches and some experimental results, the importance of: the effect of soluble silicates as an activator, the hydrothermal curing and the use of slag to reduce the efflorescence rate, is evident when used with the correct design parameters. However, it is necessary to identify the micro and nanostructural effect of the materials and the mechanisms, the relationship between design parameter and gel formed and the alkalis stability. It is also necessary to understand the carbonation process, how the pore network structure is related to external or internal crystallization, how the humidity is connected to the process and how all of these could be associated to the performance of the material in service. The effect of efflorescence formation on mechanical properties, including compressive strength, tensile strength, and linear deformation requires a greater understanding. The use of this material in civil construction requires the understanding of this phenomenon to avoid durability problems.

AUTHOR CONTRIBUTIONS

The first version of this review paper has been drafted by ZZ, and enriched by ML in 2018. ML and ZZ did all the experimental part and data analysis (collection). In the discussion part, ER and AK provided a lot of insight comments and improvements, and HW finalized the whole presentation and format of this paper. The greatest contribution of content is ML and ZZ and the rest three authors contributed equally.

ACKNOWLEDGMENTS

Funding from Australian Research Council through Discovery project (DP160104149) and DECRA (DE170101070) project are acknowledged. ML thanked the financial support of CAPES and of SWE 203750/2017-9. The participation of Brazilian authors was sponsored CNPq (Brazilian National Council for Scientific and Technological Development) through the research project UNIVERSAL grant number 458597/2014-7, as well as the research fellowships PQ2017 303753/2017-0 and 305530/2017-8. We would like to thanks the previous paper presented at the conference of the Second International Conference on Performance-based and Life-cycle Structural Engineering (PLSE 2015).

REFERENCES

Arnold, A., and Zehnder, E. K. (1989). "Salt weathering on monuments," in *I' Simposio Internazionale Bari*.

Bernal, S. A. (2016). Microstructural changes induced by CO_2 exposure in alkali-activated slag/metakaolin pastes. *Front. Mater.* 3:43. doi: 10.3389/fmats.2016.00043

Bernal, S. A., Bílek, V., and Criado, M. (2014). "Durability and testing - degradation via mass transport," in *Alkali Activated Materials: State of the Art Report*, eds por J. L. Provis and J. S. J Van Deventer (Dordrecht: Springer), 223–276.

Burciaga-Díaz, O., Escalante-Garcia, J. I., Arellano-Aguilar, R., and Gorokhovsky, A. (2010). Statistical analysis of strength development as a function of varios parameters on activated metakaolin/slag cements. *J. Am. Ceram. Soc.* 93, 541–547. doi: 10.1111/j.1551-2916.2009.03414.x

Cizer, Ö., Van Balen, K., Elsen, J., and Van Gemert, D. (2012). Real-time investigation of reaction rate and mineral phase modifications. *Constr. Build. Mater.* 35, 741–751. doi: 10.1016/j.conbuildmat.2012.04.036

Criado, M., Fernandez-Jiménez, A., and Palomo, A. (2007). Alkali activation of fly ash: effect of the SiO2/Na2O ratio. *Mocropor. Mesopor. Mater.* 106, 180–191. doi: 10.1016/j.micromeso.2007.02.055

Damtoft, J. S., Lukasik, J., Herfort, D., Sorrentino, D., and Gartner, E. M. (2008). Sustainable development and climate change initiatives. *Cement Concrete Res.* 38, 115–127. doi: 10.1016/j.cemconres.2007.09.008

Dow, C., and Glasser, F. P. (2003). Calcium carbonate efflorescence on Portland cement and building materials. *Cement Concrete Res.* 33, 147–154. doi: 10.1016/S0008-8846(02)00937-7

Duxson, P., Lukey, G. C., Separovic, F., and Deventer, J. S. J. (2005). Effect of alkali cations on aluminus incorporation in geopolymeric gels. *Ind. Eng. Chem. Res.* 44, 832–839. doi: 10.1021/ie0494216

Duxson, P., Mallicoat, S. W., Lukey, G. C., Kriven, W. M., and Van Deventer, J. S. J. (2007). The effect of alkali and Si/Al ratio on the development of mechanical properties of metakaolin-based geopolymers. *Colloids Surf.* 292, 8–20. doi: 10.1016/j.colsurfa.2006.05.044

Fernández-Jimenez, A., Palomo, A., Sobrados, I., and Sanz, J. (2006). The role played by the reactive alumina content in the alkaline activation of fly ashes. *Micropor. Mesopor. Mater.* 91, 111–119. doi: 10.1016/j.micromeso.2005.11.015

Gallucci, E., and Scrivener, K. (2007). Crystallisation of calcium hydroxide in early age model and ordinary cementitious systems. *Cement Concrete Res.* 37, 492–501. doi: 10.1016/j.cemconres.2007.01.001

Garcia-González, C. A., Hidalgo, A., Andrade, C., Alonso, M. C., Fraile, J., López-Periago, A. M., et al. (2006). Modification of composition and microstructure of Portland cement pastes as a result of natural and supercritical carbonation procedures. *Ind. Eng. Chem. Res.* 45, 4985–4992. doi: 10.1021/ie0603363

Granizo, N., Palomo, A., and Fernandez-Jiménez, A. (2014). Effect of temperature and alkaline concentration on metakaolin leaching kinetics. *Ceramics Int.* 40, 8975–8985. doi: 10.1016/j.ceramint.2014.02.071

Heath, A., Paine, K., and McManus, M. (2014). Minimising the global warming potential of clay based geopolymers. *J. Clean. Prod.* 78, 75–83. doi: 10.1016/j.jclepro.2014.04.046

Kani, E. N., Allahverdi, E. A., and Provis, J. L. (2012). Efflorescence control in geopolymers binders based on natural pozzolan. *Cement Concrete Composites* 34, 25–33. doi: 10.1016/j.cemconcomp.2011.07.007

Lloyd, R. R., Provis, J. L., and Van Deventer, J. S. J. (2010). Pore solution composition and alkali diffusion in inorganic polymer cement. *Cement Concrete Res.* 40, 1386–1392. doi: 10.1016/j.cemconres.2010.04.008

Longhi, M. A., Rodríguez, E. D., Bernal, S. A., Provis, J. L., and Kirchheim, A. P. (2016). Valorisation of a kaolin mining waste for the production of geopolymers. *J. Clean. Produc.* 115, 265–272. doi: 10.1016/j.jclepro.2015.12.011

McLellan, B. C., Williams, R. P., Lay, J., Riessen, A. V., and Corder, G. D. (2011). Costs and carbon emissions for geopolymers pastes im comparison to ordinary portland cement. *J. Clean. Prod.* 19, 1080–1090. doi: 10.1016/j.jclepro.2011.02.010

Passuelo, A., Rodríguez, E. D., Hirt, E., Longhi, M., Bernl, S. A., Provis, J. L., et al. (2017). Evaluation og the potential improvement in the environmental footprint of geopolymers using waste-derived activators. *J. Clean. Prod.* 166, 680–689. doi: 10.1016/j.jclepro.2017.08.007

Provis, J. L., and Bernal, S. A. (2014). Geopolymers and related alkali-activated material. *Ann. Rev. Mater. Res.* 44, 299–327. doi: 10.1146/annurev-matsci-070813-113515

Provis, J. L., Lukey, G. C., and Van Deventer, J. S. J. (2005). Do geopolymers actually contain nanocrystalline zeolites: a reexamination of existing results. *Chem. Mater.* 17, 3075–3085. doi: 10.1021/cm050230i

Rijniers, L. A., Huinink, H. P., Pel, L., and Kopinga, K. (2005). Experimental evidence of crystallization pressure inside porous media. *Phys. Rev. Lett.* 94, 75503–75507. doi: 10.1103/PhysRevLett.94.075503

Rowles, M. R., Hanna, J. V., Pike, K. J., Smith, M. E., and Connor, B. H. (2007). 9Si, 27Al, 1H and 23Na MAS NMR study of the bonding character in aluminosilicate inorganic polymers. *Appl. Magnet. Ressonance* 32, 663–687. doi: 10.1007/s00723-007-0043-y

Rowles, M. R., and O'Connor, B. (2003). Chemical optimisation of the compressive strength of aluminosilicate geopolymers synthesised by sodium silicate activation of metakaolinite. *J. Mater. Chem.* 13, 1161–1165. doi: 10.1039/b212629j

San Nicolas, R., and Provis, J. L. (2015). The interfacial transition zone in alkali-activated slag mortars. *Front. Mater.* 2:70. doi: 10.3389/fmats.2015.00070

Šavija, B., and Lukovic, M. (2016). Carbonation of cement paste: understanding, challenge and opportunities. *Construc. Build. Mater.* 117, 285–301. doi: 10.1016/j.conbuildmat.2016.04.138

Scherer, G. W. (2004). Stress from crystallization of salt. *Cement Concrete Res.* 34, 1613–1624. doi: 10.1016/j.cemconres.2003.12.034

Shen, W., Wang, Y., Zhang, T., Zhou, M., Li, J., and Cui, X. (2011). Magnesia modification of alkali-activated slag fly ash cement. *J. Wuhan Univer. Tech. Mater.* 26, 121–125. doi: 10.1007/s11595-011-0182-8

Škvára, F., Kopecký, L., Mysková, L., Smilauer, V., Alberovská, L., and Vinsová, L. (2009). Aluminosilicate polymers - influence of elevated temperatures, efflorescence. *Ceram. Silikáty* 53, 276–282.

Škvára, F., Kopecký, L., Nemecek, J., and Bittnar, Z. (2006). Microstructure of geopolymer materials based on fly ash. *Ceram. Silikaty* 50, 208–215.

Škvára, F., Šmilauer, V., Hlavácek, P., Kopecky, L., and Cilová, Z. (2012). A weak alkali bond in (N, K)-A-S-H gels: evidende from leaching and modeling. *Ceram. Silikáty* 56, 374–382.

Temuujin, J., Minjigmaa, A., Lee, M., Chen-Tan, N., and van Riessen, A. (2011). Characterization of glass F fly ash geopolymer pastes immersed in acid and alkali solutions. *Cement Concrete Composites* 33, 1086–1091. doi: 10.1016/j.cemconcomp.2011.08.008

Van Deventer, J. S. J., Lukey, G. C., and Xu, H. (2006). Effect of curing temperature and silicate concentration on fly-ash-based geopolymerization. *Ind. Eng. Chem. Res.* 45, 3559–3568. doi: 10.1021/ie051251p

Van Deventer, J. S. J., Provis, J. L., and Duxson, P. (2012). Technical and commercial progress in the adoption of geopolymer cement. *Miner. Eng.* 29, 89–104. doi: 10.1016/j.mineng.2011.09.009

Yao, X., Yang, T., and Zhang, Z. (2015). Compressive strength development and shrinkage of alkali-activated fly ash-slag blends associated with efflorescence. *Mater. Struct.* 49, 2907–2918. doi: 10.1617/s11527-015-0694-3

Zhang, D., Ghouleh, Z., and Shao, Y. (2017). Review on carbonation curing of cement-bases materials. *J. CO_2 Utilizat.* 21, 119–131. doi: 10.1016/j.jcou.2017.07.003

Zhang, X., Glasser, F. P., and Scrivener, K. L. (2014a). Reaction kinetics of dolomite and portlandite. *Cement Concrete Res.* 66, 11–18. doi: 10.1016/j.cemconres.2014.07.017

Zhang, Z., Provis, J. L., Ma, X., Reid, A., and Wang, H. (2018). Efflorescence and subflorescence induced microstructural and mechanical evolution in fly ash-based geopolymers. *Cement Concrete Composit.* 92, 165–177. doi: 10.1016/j.cemconcomp.2018.06.010

Zhang, Z., Provis, J. L., Reid, A., and Wang, H. (2014c). Fly Ash-based geopolymers: the relation between composition, pore structure ans eflforescence. *Cement Concrete Res.* 64, 30–41. doi: 10.1016/j.cemconres.2014.06.004

Zhang, Z., Provis, J. L., Wang, H., Bullen, F., and Reid, A. (2013). Quantitative kinetic and structural analysis of geopolymers. Part 2. Thermodynamics of sodium silicate activation of metakaolin. *Thermochim. Acta* 565, 163–171. doi: 10.1016/j.tca.2013.01.040

Zhang, Z., and Wang, H. (2016). The pore characteristics of geopolymer foam concrete and their impact on the compressive strength and modulus. *Front. Mater.* 3:38. doi: 10.3389/fmats.2016.00038

Zhang, Z., Wang, H., Zhu, Y., Reid, A., and Provis, J. L. (2014b). Using fly ash to partially substitute metakaolin in geopolymer synthesis. *Appl. Clay Sci.* 88–89, 194–201. doi: 10.1016/j.clay.2013.12.025

Zhang, Z., Yao, X., and Zhu, H. (2012). Potential application of geopolymers as protection coatings for marine concrete III. Field experiment. *Appl. Clay Sci.* 67–68, 57–60. doi: 10.1016/j.clay.2012.05.008

Conflict of Interest Statement: The authors declare that the research was conducted in the absence of any commercial or financial relationships that could be construed as a potential conflict of interest.